

# **Simulations of HL-LHC Crab Cavity Noise using HEADTAIL**

A Senior Project

presented to

the Faculty of the Physics Department

California Polytechnic State University, San Luis Obispo

In Partial Fulfillment

of the Requirements for the Degree

Bachelors of Science

by

Stan Steeper

September 2015

© 2015 Stan Steeper

# Simulations of HL-LHC Crab Cavity Noise using HEADTAIL

Stan Steeper

September 11, 2015

## Abstract

The High Luminosity Large Hadron Collider (Hi-Lumi LHC) upgrade – scheduled to be completed by 2025 – will improve the existing LHC in many ways. One such upgrade is the addition of Crab Cavities (CCs). The CCs are resonant structures that provide strong transverse kicks to the circulating clouds of particles around each interaction region. As such, the CCs result in a head-on collision of the clouds and a large increase in event rate, leading to reduced statistical uncertainty and potentially faster discoveries. However, the CC field will be modulated by phase and amplitude noise which can have detrimental effects on beam quality. Of utmost concern is the increase in the particle cloud transverse size due to the noise action, which can lead to reduced collision rates or even loss of particles. The relationship between the noise spectrum and the size growth rate has been quantified with a theoretical model [1]. This work presents simulation results using the Python multi-particle tracking package HEADTAIL to validate this model. The evolution of the particle cloud transverse distribution due to the noise is also investigated via HEADTAIL.

## 1 Introduction

### 1.1 Background

The Crab Cavity (CC) mechanism is one of several upgrades planned for the High Luminosity Large Hadron Collider (HL-LHC). The purpose of the CC is to provide a strong transverse magnetic kick to the protons before the beam crossing point (the target), with the effect of orienting the bunches into better collision position. Because the bunches are 4 orders of magnitude larger along the longitudinal axis than the transverse axis, reducing the crossing angle to as close to zero as possible increases the overlap of the colliding bunches significantly. (Fig. 1). A better overlap gives a higher luminosity (a number of collisions per area per time), which leads to a higher event rate allowing for quicker discoveries and less statistical uncertainty in identifying particles.

The present-day nominal LHC collides clouds of  $10^{11}$  protons called bunches traveling at  $v = .99999999c$  ( $\gamma = 7460$ ,  $E = 6.5$  TeV). There are 2808 7.5cm long bunches in a full intensity beam, and are spaced about 7.5m or 25ns apart. At full speed, the bunches hit the collision point with revolution frequency  $f_{rev} = 11245$  Hz, with only about 20 protons interacting per turn, giving about 600 million collisions per second [2]. The HL-LHC design will improve the luminosity by a factor of 10 [3].

The bunches travel in the circular  $s$  direction (the longitudinal axis) and also have small  $x$  and  $y$  (transverse) motion. The synchronous particle is defined as a theoretical particle that arrives precisely on time with respect to the RF cavity (the accelerating voltage) signal. A statistical representation of the bunch of particles is used for a theoretical model of the beam dynamics. The symbols  $x_{max}$ ,  $\nu_b$ , and  $\theta$  are associated with the transverse plane and refer to the peak amplitude of oscillation, the tune (the FWHM of the velocity distribution), and the phase respectively. Similarly  $\phi_{max}$ ,  $\nu_s$ , and  $\psi$  refer to the peak amplitude, tune, and phase in the longitudinal axis. The transverse motion is called betatron oscillation and has frequency  $f_b$ , while the longitudinal motion is called the synchrotron oscillation with frequency  $f_s$ . The tunes are defined as  $\nu_b = f_b/f_{rev}$  and  $\nu_s = f_s/f_{rev}$ .

### 1.2 The Effect of Crab Cavity Noise

There is a downside to the addition of Crab Cavities – the CC signal carries noise that can negatively affect the beam quality. Specifically, the power supplied by the noise can cause an increasing transverse

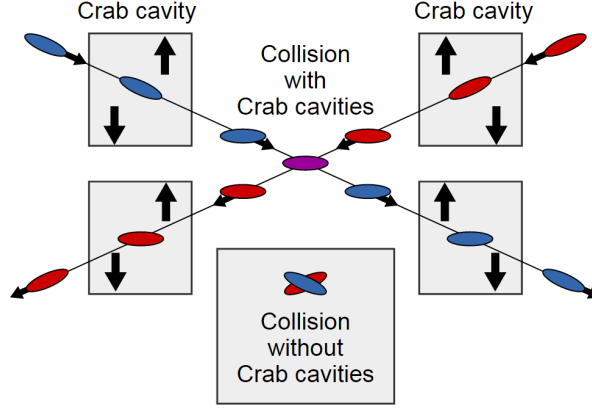


Figure 1: The four Crab Cavities kick the head of the bunch upward and the tail of the bunch downward, flattening out the bunch right before collision at center. Without the CC, the bunches have less overlap and as a consequence fewer collision events occur. (Image source: [http://en.wikipedia.org/wiki/Crab\\_cavity](http://en.wikipedia.org/wiki/Crab_cavity))

emittance of the bunches over time. The emittance is defined as the area of the bunch in phase space (see Fig. 2). A higher emittance corresponds to higher variation from the ideal position, negatively affecting the luminosity and also leading to particle loss. The dependence of the emittance growth rate on the power of the noise is quantified by using a mathematical theory, and numerical simulations are used to confirm the theoretical model. Using this knowledge, a design limit on the power of the noise can be established so that the emittance growth stays under a specified rate.

The effect of the noise can be modeled as momentum kicks through the relation

$$\Delta p = \frac{eV}{c} \quad (1)$$

The noisy signal takes the form  $V = V_0(1 + \Delta A)\sin(\phi_n + \Delta\phi_n)$  with  $V_0$  the CC voltage,  $\phi_n$  the phase of the particle on turn with respect to the synchronous particle (the theoretical particle that arrives precisely at the right time),  $\Delta\phi_n$  the phase noise, and  $\Delta A$  the relative amplitude noise (Fig. 3 illustrates the difference between  $\Delta A$  and  $\Delta\phi$ ). Using Eq. 1, it is possible to derive the momentum kicks from the noisy CC signal [1]. For phase noise,

$$\Delta p_\phi = -\sqrt{\beta_{CC}} \frac{eV_0}{E} \cos(\phi_{max}\sin(2\pi n\nu_s + \psi)) \Delta\phi_n \quad (2)$$

and for amplitude noise:

$$\Delta p_A = -\sqrt{\beta_{CC}} \frac{eV_0}{E} \sin(\phi_{max}\sin(2\pi n\nu_s + \psi)) \Delta A_n \quad (3)$$

where  $\beta_{CC}$  is a parameter related to the magnetic field strength at the CC. The important distinction between  $\Delta p_\phi$  and  $\Delta p_A$  is the dependence on the synchrotron motion, through cosine for phase noise and sine for amplitude noise. Assuming a short longitudinal bunch length, the phase noise momentum kick will be uniform across the length of the bunch, whereas the amplitude noise momentum kick will be nearly zero. With longer bunch lengths,  $\Delta p_\phi$  is reduced towards the head and tail of the bunch, whereas  $\Delta p_A$  will become nonzero and increase towards the head and tail.

A particle in an accelerator has transverse motion that can be described using the Hamiltonian formalism:

$$x = \beta \frac{dp}{ds} \quad (4)$$

$$p = \beta \frac{dx}{ds} \quad (5)$$

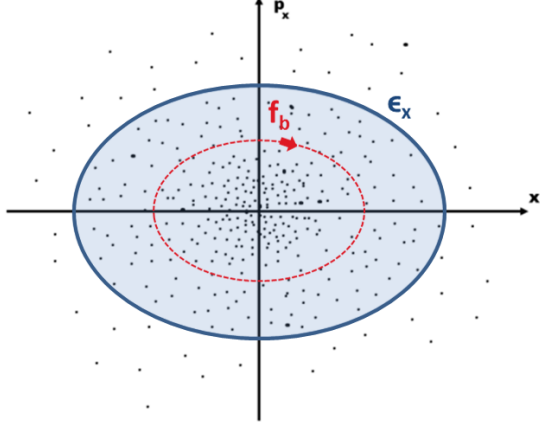


Figure 2: A representation of the transverse emittance as the area of the bunch (here defined as 95% inclusion of the particles) in phase space. Particles rotate in this space with frequency  $f_b$ .

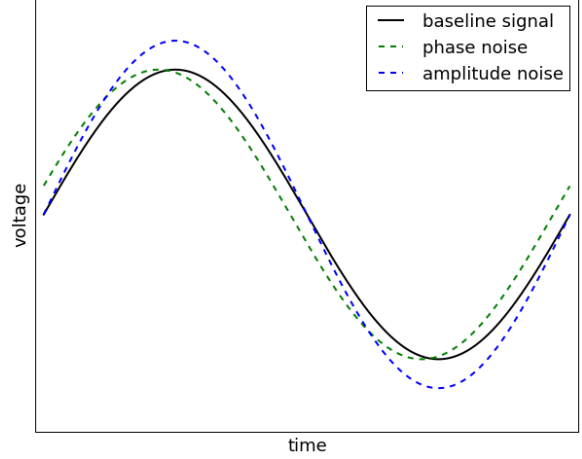


Figure 3: A conceptual diagram showing the difference between phase and amplitude noise. Note that phase noise shifts the signal horizontally, and amplitude noise stretches the signal vertically.

which represents circular motion in a normalized phase space. In this system, the emittance is defined as

$$\epsilon = \frac{1}{2}(E[(x - E[x])^2] + E[(p - E[p])^2]) \quad (6)$$

where  $E[X] = \int_{-\infty}^{\infty} xf(x)dx$  is the expected value of  $x$  assuming the distribution  $X$  has a probability density function  $f(x)$ . Because the phase space is normalized, (6) can be written

$$\epsilon = E[(x - E[x])^2] = E[(p - E[p])^2] \quad (7)$$

The oscillations are symmetric about the origin, meaning  $E[x] = 0$ , leaving

$$\epsilon = E[x^2] \quad (8)$$

which is an important and useful result for tracking the emittance growth rate.

### 1.3 Emittance Growth Rate Dependence on Power

Using Eq. 8 along with Eqs 4 and 5 the emittance growth rate due to phase and amplitude noise can be derived [1]. For phase noise the result is

$$\frac{d\epsilon_x}{dt} = \beta_{CC} \left( \frac{eV_0 f_{rev}}{2E} \right)^2 C_1(\sigma_\phi) \sum_{k=-\infty}^{\infty} S_{\Delta\phi}[(k \pm \nu_b) f_{rev}] \quad (9)$$

For amplitude noise, the rate is:

$$\frac{d\epsilon_x}{dt} = \beta_{CC} \left( \frac{eV_0 f_{rev}}{2E} \right)^2 C_2(\sigma_\phi) \sum_{k=-\infty}^{\infty} S_{\Delta A}[(k \pm \nu_b \pm \nu_s) f_{rev}] \quad (10)$$

There is a lot to unpack here. To start, both rates are linearly proportional to the beta function at the CC and quadratically dependent on the quantity  $eV_0 f_{rev}/2E$ . These parameters will stay constant throughout the simulations presented in this paper, as they are never changed for normal LHC operation. The energy of the particles,  $E$ , of course increases as the particles are accelerated, but CC collisions only begin happening once the particles have been accelerated to the operating energy, which then remains constant for the whole run. The summation term at the end of Eq. 9 implies that the growth rate is linearly dependent on  $S(f)$ , the Power Spectral Density (PSD) of the noise – specifically the parts of the PSD that overlap with the betatron frequency  $f_b$  (because  $\nu_b f_{rev} = f_b$ ). For Eq. 10 the relevant

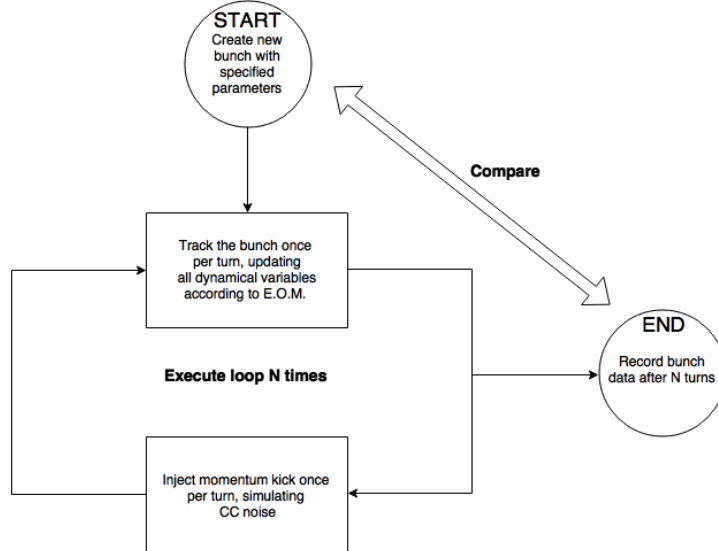


Figure 4: A block diagram illustrating how HEADTAIL is used to simulate the effect of Crab Cavity noise. At start, a normally distributed bunch is created with parameters chosen to represent the HL-LHC operating point. The bunch is tracked for  $N$  turns, receiving a momentum kick on each turn. Data is logged from the bunch at the end of the run, and the starting and ending bunch distributions can be directly compared.

frequencies are the parts of the PSD that overlap with the sum of  $f_b$  and  $f_s$ . The PSD is the Fourier transform of the noise time signal, giving the power as a function of frequency. Lastly, there are correction factors,  $C_1$  and  $C_2$ , that depend on  $\sigma_\phi$  which is the bunch length represented as the standard deviation with respect to  $\phi$ , the synchrotron phase. The correction factors are

$$C_1(\sigma_\phi) = e^{-\sigma_\phi^2} \left[ J_0(\sigma_\phi^2) + 2 \sum_{n=1}^{\infty} J_{2n}(\sigma_\phi^2) \right] \quad (11)$$

$$C_2(\sigma_\phi) = e^{-\sigma_\phi^2} \sum_{n=0}^{\infty} J_{2n+1}(\sigma_\phi^2) \quad (12)$$

where  $J_n$  are the Bessel functions of the first kind.

## 1.4 HEADTAIL

The Python package PyHEADTAIL is a multi-particle beam dynamics simulation package. It has been used extensively in a research setting at CERN and elsewhere, and its validity as a computational tool is well established. The user can input the beam parameters from the LHC and simulate a beam in the presence of both phase and amplitude noise – see Fig. 4 for a diagram of the process. The bunches containing approximately  $10^5$  simulated particles receive momentum kicks once per turn and the emittance is tracked over timescales of  $10^5$  turns. The revolution frequency of the LHC is  $f_{rev} = 11245$  Hz, so the order of  $10^5$  turns corresponds to the order of 10 seconds of real time.

HEADTAIL supports the inclusion of a transverse damper. The damper acts on the mean position of the bunch ( $\approx 0$ ) and reduces the transverse oscillations of the bunch. The gain of the damper is adjustable, with higher gains being more effective at reducing the emittance growth rate.

## 1.5 Stochastic Cooling

The transverse damper acts only on the mean of the particles' position so theoretically it cannot reduce the transverse emittance. However, in simulation with low numbers of particles ( $10^5$  is used for most runs compared to  $10^{11}$  in the LHC), the damper can act like a stochastic cooling system (SCS) and

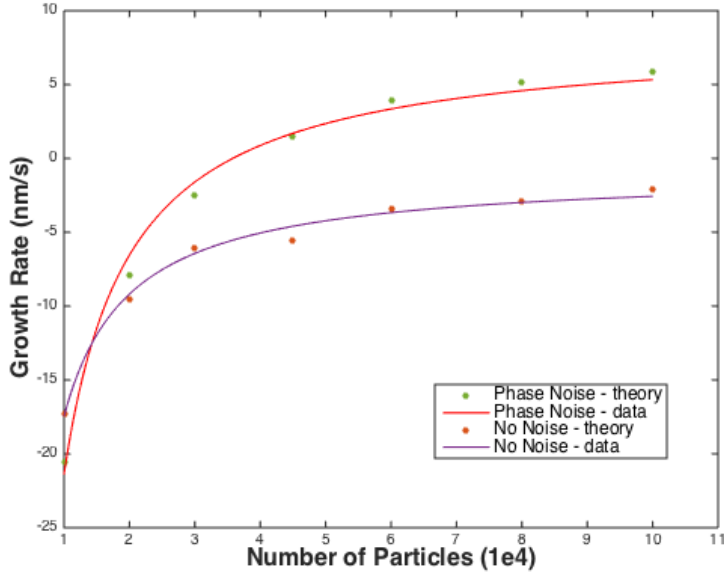


Figure 5: The stochastic cooling rate is only significant for low  $N$ . In the LHC,  $N \approx 10^{11}$ , so no stochastic cooling effect is present for the real beam. For all simulations, the number of particles was high enough so that the stochastic cooling rate was at least an order of magnitude smaller than the noise-induced emittance growth rate.

reduce the transverse variance of the bunch [4]. The reason a SCS can reduce the variance is because it can act with varying strength on particles of varying oscillation amplitudes. At low  $N$ , the particles are not well mixed, leading to a nonzero mean, with the highest contributions to the mean being the particles with the greatest amplitude. The damper acts on these particles preferentially and in doing so can reduce the variance and consequently the emittance over time. In the absence of noise we see a negative emittance growth rate as a result (see Fig. 5). This means that the number of particles must be increased until the effect is negligible.

## 2 Results

Simulations were run with varying parameters, most importantly the presence or absence of a transverse damper, the number of particles  $N$ , longitudinal bunch length  $\sigma_z$ , and the amplitude  $A$  and type of noise (amplitude or phase). The effect on the emittance growth rate for each of these parameters is simulated.

### 2.1 Amplitude and PSD dependence

Equations 9 and 10 imply that the emittance growth rate is linearly proportional to the PSD around  $f_b$ . In order to vary the power of the noise in the HEADTAIL code, we vary the amplitude of the momentum kicks. The PSD of the noise is proportional to the square of the amplitude.

The amplitudes varied in the code are converted to PSD and emittance growth rate as a function of PSD is plotted in Fig 6. The solid line is theory and each data point is the average of the results of 10 identical runs, with standard deviations on the error bars.

### 2.2 Longitudinal Bunch Length dependence

As mentioned in section 1.3, the emittance growth rate depends on the longitudinal bunch length through the correction factors in Eqs. 11 and 12. For amplitude noise, the factor is 0 for small bunch lengths and increases with bunch length to a maximum of .25. For phase noise, the factor is 1 for small bunch lengths and drops off to .5 as bunch length increases.

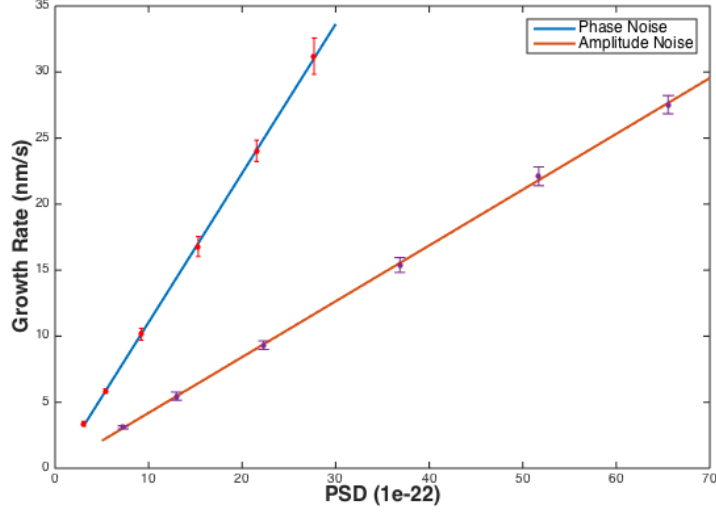


Figure 6: The emittance growth rate as a function of PSD for both phase and amplitude noise are plotted. Multiple simulations were run for each data point and the errorbars denote the standard deviation.

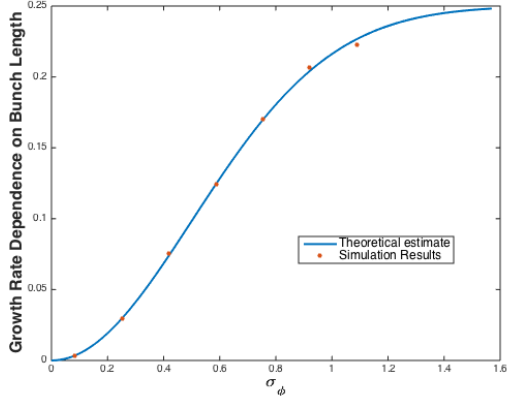


Figure 7: The correction factor as a function of bunch length for amplitude noise.

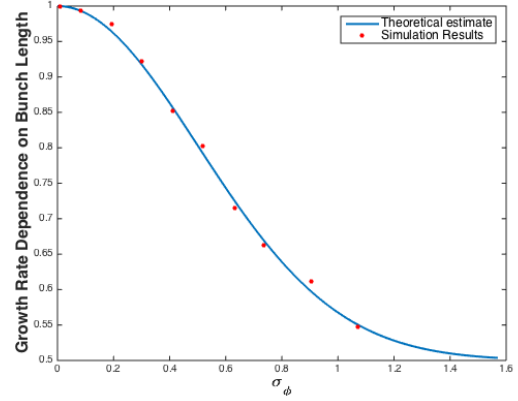


Figure 8: The correction factor as a function of bunch length for phase noise.

Simulations were run with both phase and amplitude noise with constant noise power. The bunch length was varied in order to observe the effect on the emittance growth rate. The simulation data points are shown in Figures 7 and 8, on top of the theoretical model prediction. The bunch length is represented as  $\sigma_\phi$ , or the standard deviation with respect to the synchrotron phase. In the HL-LHC, the expected bunch length is  $\sigma_\phi = .6325$ .

### 2.3 Transverse Damper effects

The damper acts to reduce the transverse oscillations of the bunch and consequently the emittance growth rate. The correction factor for the effect of the damper depends on the damper gain and the betatron tune distribution. The parameter  $\alpha = G/4\pi\sigma_{\nu_b}$  relates the damper gain  $G$  to the betatron tune spread  $\sigma_{\nu_b}$ . The correction factor can then be quantified as a function of  $\alpha$  for each tune distribution. Two such plots are shown in Figures 9 and 10.

Simulations were run with varied damping rate and all other parameters constant. For short bunch lengths, the results agree well. The model for long bunch lengths is currently being developed.

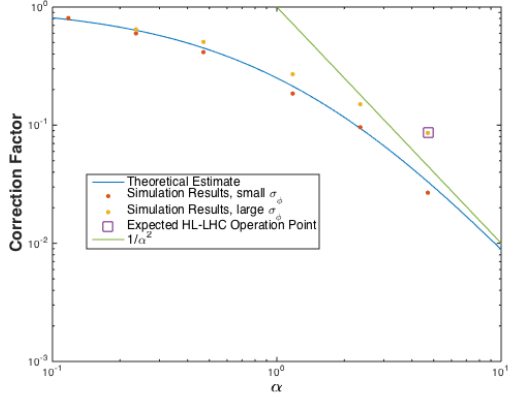


Figure 9: Comparison of theory and simulation for a gaussian tune distribution (the red curve of Fig. 11). The planned HL-LHC operation point is marked. The correction factor asymptotically approaches  $1/\alpha^2$  as  $\alpha$  increases.

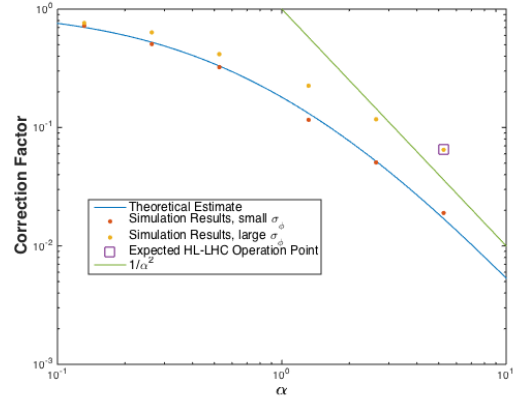


Figure 10: Comparison of theory and simulation for the expected HL-LHC tune distribution (the dark blue curve of Fig. 11).

### 3 Position and Tune Distribution Evolution over Long Runs

So far, this paper has focused on the emittance growth rate over the course of a simulation. The emittance is a useful parameter to monitor, but it reduces the complex dynamics of the bunch to a single number. In order to gain more information, it makes sense to observe the effect of the noise on the betatron tune distribution and the transverse position distribution. If the CC noise has the effect of modifying these distributions, it is possible that it will have a negative effect on beam quality. The transverse position distribution is ideally gaussian. If it deviates from normal, it can have negative consequences for beam interaction with the machine impedance.

Simulations were run for a range of betatron tune distributions, shown in Fig 11. The position distributions all start the same, as gaussian. Prolonged CC noise over  $10^6$  turns was simulated for each distribution and the ending distributions were compared to the starting distributions.

The results show that when the power of the CC noise is high enough, the position distribution at the end of the noisy run is still gaussian, but that the particles spread out to higher distances over time (which is expected for increasing emittance). The betatron tune distribution evolves over time as well, showing a trend toward higher frequencies. The following plots show simulation data displaying the effect of sustained noise on the position and betatron distributions. The changes observed in these two position distributions are dependent on the noise level as well as the starting tune distribution. Figures 12-17 show data from high-noise runs with  $\text{PSD} = 16 \times 10^{-22} \text{ rad}^2 \text{ Hz}^{-1}$ ,  $N = 10^6$  turns and starting emittance  $\epsilon_x = 2.5 \mu\text{m}$ . There is a pair of plots for each of three cases showing the starting and ending position distribution on the left and the starting and ending tune distribution on the right. The data for the expected distribution (dark blue in Fig 11) is shown first, and then the two limiting tune distributions are shown (green and red in Fig 11).

Figures 12 through 17 suggest that bunches with different starting betatron tune distributions are affected differently by the CC noise. With noise power held constant, the high chromaticity gaussian bunch sees a smaller emittance growth and only minor changes to the position and tune distributions compared to the expected tune distribution in Fig. 12. A possible explanation for this observation is that the high chromaticity bunch has a stronger transverse-longitudinal coupling, meaning a large part of the noise energy is transferred to the longitudinal motion of the bunch. More data is needed to confirm and quantify this theory.

The Fourier transform of the position histogram data was also obtained in order to check for any noticeable deviations between starting and ending distributions. A gaussian distribution under a Fourier transform remains gaussian, but it is sometimes easier to identify any small deviations from gaussian in Fourier space. From the transform plots in Figures 18 and 19, there are a negligible amount of particles



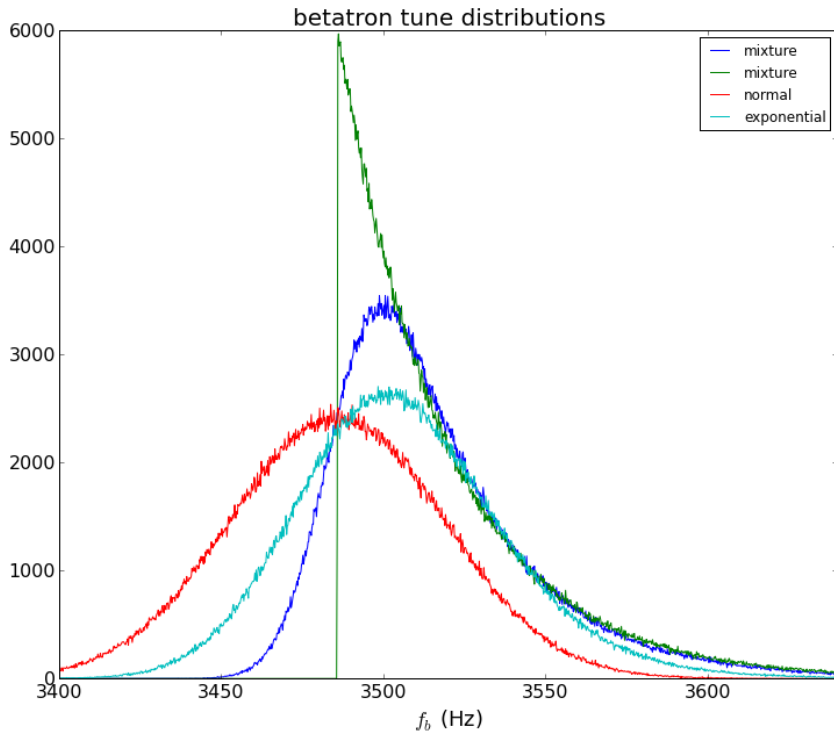


Figure 11: The four different betatron tune distributions used for long runs. The green exponential and red normal distributions are limiting cases corresponding to various combinations of quadrupole/octopole terms in the multipole expansion of the steering magnetic field. In the LHC the distribution will be somewhere in between the two, close to the dark blue distribution.

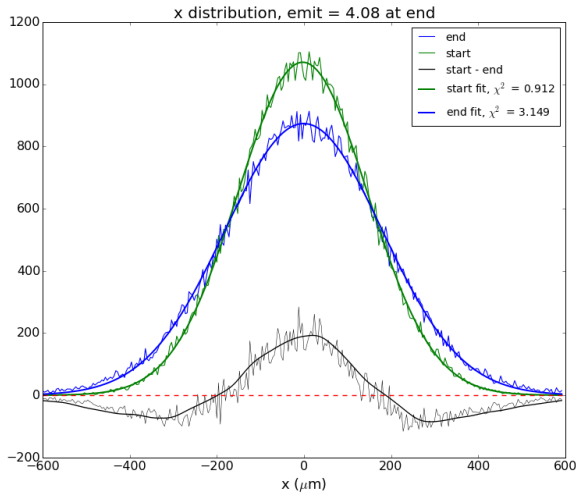


Figure 12: The first case, with tune distribution at right. The emittance started at  $2.5 \mu\text{m}$  and ended at  $4.08 \mu\text{m}$ , or an emittance growth rate of  $18 \text{ nm/s}$ . The change in width of the gaussian is  $\Delta\sigma = 31 \mu\text{m}$ .

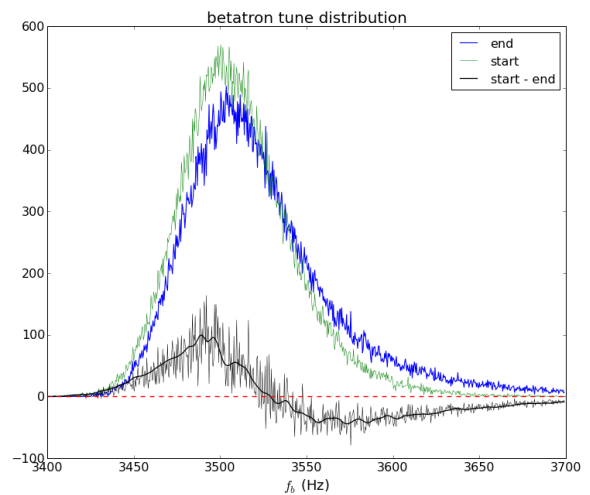


Figure 13: The betatron tune distribution at the start and finish of a high-noise run. The peak flattens out and particles shift towards higher  $f_b$ .

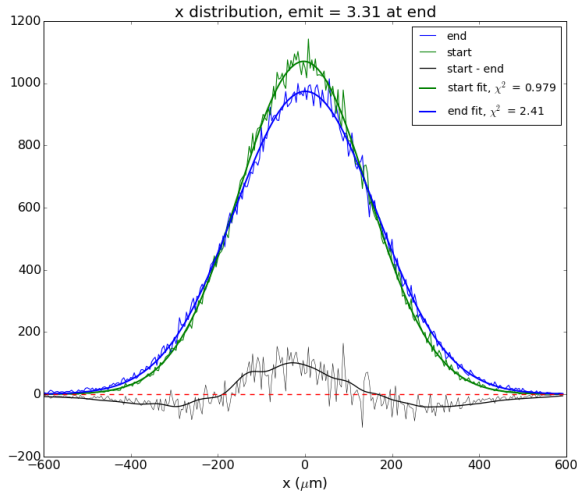


Figure 14: The gaussian tune distribution case. The position distribution is not modified by the noise as much as in Fig. 12. The emittance growth rate is smaller for this case at 9 nm/s. The change in width of the gaussian is  $\Delta\sigma = 14\mu\text{m}$ .

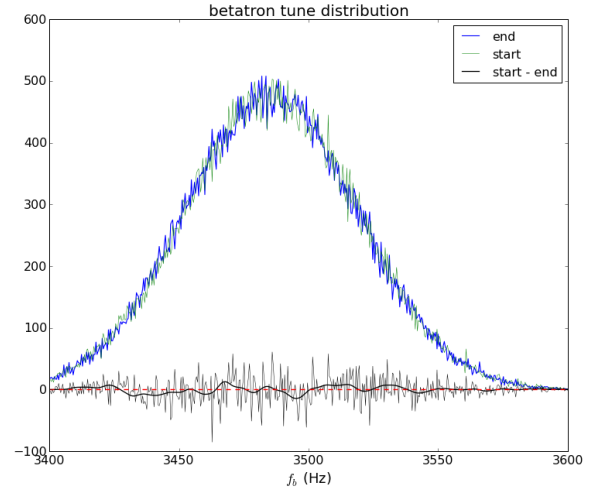


Figure 15: The symmetric gaussian betatron tune distribution remains unchanged by the high noise run, suggesting this distribution is more resilient to the effect of CC noise on transverse motion.

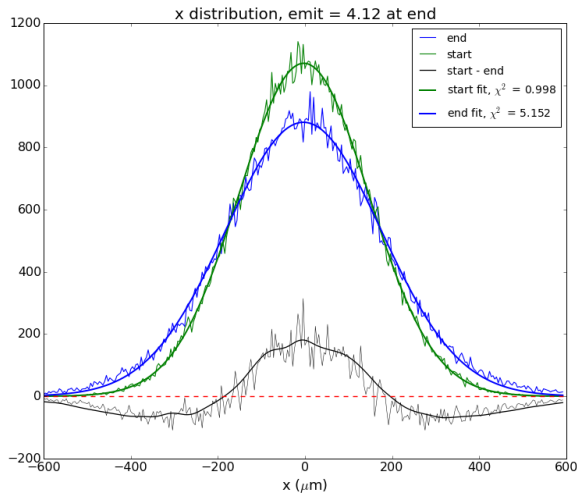


Figure 16: The exponential tune distribution case. The emittance growth rate and the effect on the position distribution is about the same for this case as the expected case:  $d\epsilon/dt = 19 \text{ nm/s}$ ,  $\Delta\sigma = 29\mu\text{m}$ .

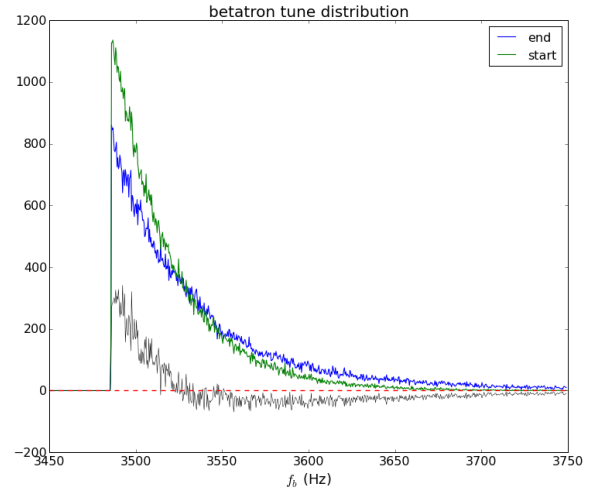


Figure 17: The exponential betatron tune distribution sees a shift towards higher frequencies as a result of the CC noise.

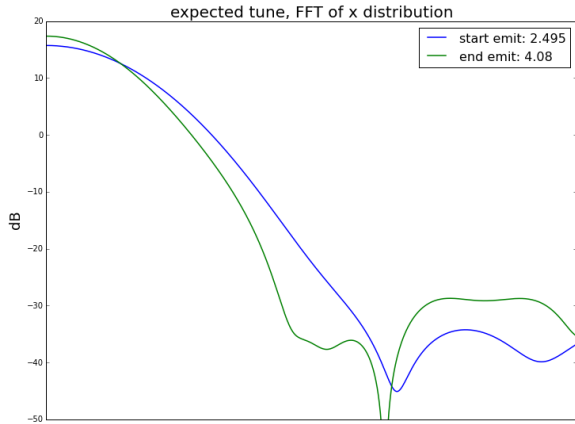


Figure 18: The Fourier transform of the position distribution for the expected tune case. As expected, the width of the gaussian decreases in Fourier space as it increase in position space. Any higher frequency content outside of the gaussian curve is at about -30 dB.

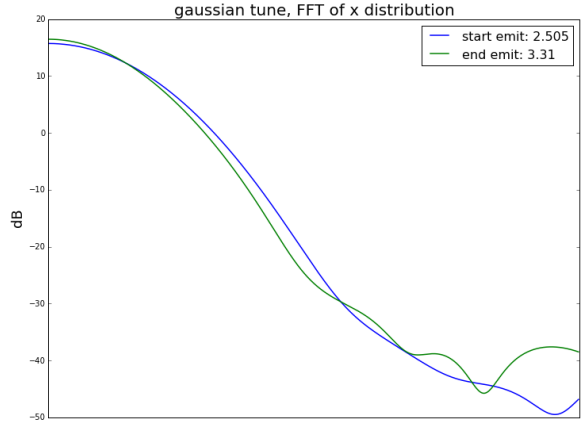


Figure 19: The Fourier transform of the position distribution for the gaussian tune case. Again, all higher frequency noise outside of the curve is at the -30 dB level. It is clear that the gaussian betatron tune bunches see less of an effect on transverse position.

outside of the gaussian shape – the noise is on the order of -30 dB.

## 4 Tail Cleaning with Crab Cavity Noise

In the previous section, the transverse position distribution only increased in width due to the CC noise; no change in shape occurred. It is possible, however, to use the CC noise as a "tail cleaning" mechanism. Tail cleaning is the process by which particles with high transverse position are ejected from the bunch and are scraped away with a collimator, resulting in a more compact and stable bunch. In order to produce this effect, noise with narrow spectral content inside the tune distribution is injected.

The feasibility of using Crab Cavity noise for this purpose was tested in simulation. As opposed to the white noise in section 3, simulations were run with narrowband noise of bandwidth 6 Hz, and also "monochromatic" noise consisting of a single frequency. To produce the tail cleaning effect on the transverse distribution, the noise was centered at 3670 Hz or higher. In addition, particles outside of a threshold range were placed at large transverse positions, reproducing the effect of a physical collimator. In the simulation code, on every turn the  $x$  position of each particle is checked and is redefined as  $\pm x_{large}$  if it is outside of a threshold range, effectively removing the particle from the bunch. A threshold value of  $750\mu m$  or higher is used in the simulation code, modeling the physical collimator in the LHC. The arbitrary value  $x_{large} = 5000\mu m$  is used in the simulations.

This approach is generalized to include the  $y$  dimension. Because of the difference in the transverse tunes  $Q_x$  and  $Q_y$ , the noise center frequency in  $y$  is shifted up 110 Hz relative to the noise center frequency in  $x$ . The collimation is modeled as octagonal: a particle is ejected from the bunch if it satisfies the condition ( $|x| > \text{threshold}$  OR  $|y| > \text{threshold}$  OR  $|x + y| > \text{threshold}$ ). The tune footprint, a two dimensional histogram of the horizontal and vertical betatron frequency distribution, is a useful visualization of the transverse dynamics. The footprint for a bunch at the start of a run is shown in Figure 20. At the end of the run, a successful tail cleaning would remove particles at high horizontal and vertical frequencies. The effect of injecting noise and collimating particles in only the x dimension is shown in Figure 21.

The results of these simulations show that selectively modifying the final transverse distribution by injecting narrowband noise of varying frequency is possible, but that too many particles are lost to the collimator for this strategy to represent a practical method of tail cleaning. For example, we begin to see the desired effect for short simulations (10,000 turns) with high noise amplitude as in Figure 22, but the collimator has removed 17% of the particles in less than one second of real time. In Figure 23, the effect on the transverse tune distribution is shown.

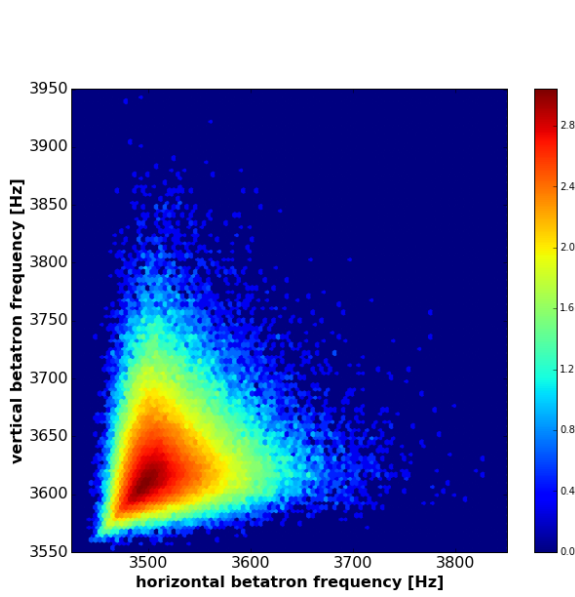


Figure 20: The tune footprint at the start of a run. The color scale is logarithmic.

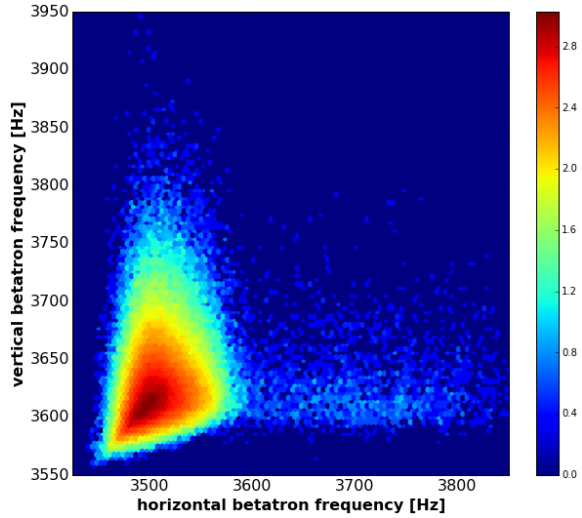


Figure 21: The tune footprint (log color scale) at the end of a run with noise and collimation in only the  $x$  dimension. Noise of frequency 3690 Hz was injected and the collimation threshold is at  $750\mu\text{m}$ . The horizontal edge of the footprint is shaved off after the run, but a sparse trail of particles extend out to about 3800 Hz.

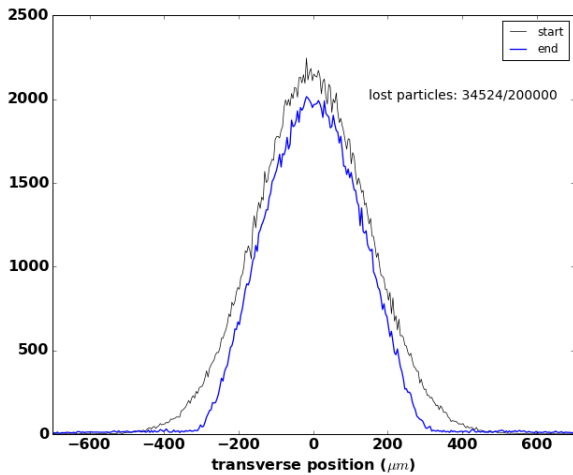


Figure 22: The effect of a high noise, low number of turns simulation on transverse tune. Filtered end of the same run as left. Note that even though noise of bandwidth 6 Hz and center frequency 3690 Hz with a collimator threshold of  $\pm 750\mu\text{m}$  was used for this run.

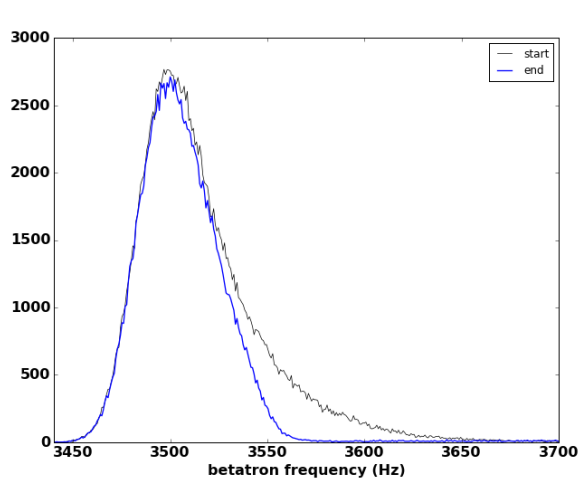


Figure 23: The tune distribution at the start and end of the same run as left. Note that even though noise of bandwidth 6 Hz and center frequency 3690 Hz with a collimator threshold of  $\pm 750\mu\text{m}$  was used for this run.

To attempt to preserve a high particle count while achieving a tail cleaning effect, the noise amplitude is lowered and the number of turns is increased. Still, a significant number of particles are lost from the core of the bunch before any tail cleaning effect is achieved. In Figure 24, the effect of monochromatic noise at  $f = 3690$  Hz over 875,000 turns (78 sec) with a larger collimator threshold of  $\pm 900\mu\text{m}$  is shown. About 3% of particles are lost, and the tails are not cleaned so much as smeared out – more particles are outside of  $3\sigma$  at the end of the run than at the start.

A range of noise frequencies were simulated, from which it was determined that higher frequencies in the 3700-3730 Hz range work better for selectively targeting particles in the tails of the transverse

distribution and at the high end of the tune distribution. Note that these frequencies are outside of the tune distribution, but that particles are still being affected by the noise. In fact, particles with betatron frequency about 150 Hz lower than the noise frequency are affected.

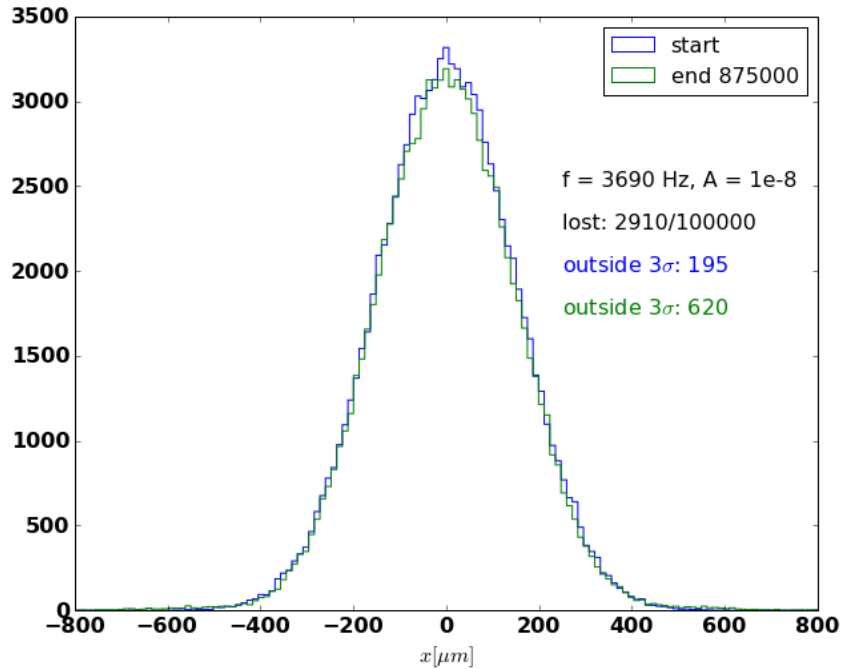


Figure 24: A low noise, long run shows no evidence of the desired tail cleaning effect. Particles are pushed to higher transverse positions without getting effectively cleaned by the collimator.

## 5 Conclusion

The results in this report demonstrate an understanding of the emittance growth dynamics as a function of several parameters. No significant discrepancy between simulation and theory has been found. The evolution of the position and betatron tune distributions due to the effect of Crab Cavity noise was simulated. A tune distribution dependent effect was observed, This work helps to build confidence towards an understanding of the Crab Cavity noise effect on beam dynamics. Future work on this topic will involve quantifying the evolution of the position and tune distribution as presented in section 3.

In terms of attempting to achieve a realistic tail cleaning method, this work presents a first approach. The proof of concept was presented, showing that CC noise can selectively modify the transverse position and tune distributions. However, future work will be necessary in order to find parameters that retain high particle counts while still achieving the desired effect. Ongoing experiments at the LHC provide insight into this process. Noise with time-varying frequency will be simulated in attempts to produce the tail cleaning effect.

## 6 References

- [1] T. Mastoridis, P. Baudrenghien, "Transverse emittance growth due to RF noise in the Hi-Lumi LHC Crab Cavities"
- [2] <http://lhc-machine-outreach.web.cern.ch/lhc-machine-outreach/collisions.htm>
- [3] <http://hilumilhc.web.cern.ch/>
- [4] <http://home.web.cern.ch/about/engineering/stochastic-cooling>